

## Charm production in high multiplicity pp events

K. Werner<sup>(a)</sup>, B. Guiot<sup>(a,b)</sup>, Iu. Karpenko<sup>(c,d,e)</sup>, T. Pierog<sup>(f)</sup>, G. Sophys<sup>(a)</sup>

<sup>(a)</sup> SUBATECH, University of Nantes – IN2P3/CNRS– EMN, Nantes, France

<sup>(b)</sup> Universidad Técnica Federico Santa María, Valparaiso, Chile

<sup>(c)</sup> FIAS, Johann Wolfgang Goethe Universität, Frankfurt am Main, Germany

<sup>(d)</sup> Bogolyubov Institute for Theoretical Physics, Kiev 143, 03680, Ukraine

<sup>(e)</sup> INFN - Sezione di Firenze, Via G. Sansone 1, I-50019 Sesto Fiorentino (Firenze), Italy and

<sup>(f)</sup> Karlsruhe Inst. of Technology, KIT, Campus North, Inst. f. Kernphysik, Germany

Recent experimental studies of the multiplicity dependence of heavy quark (HQ) production in proton-proton collisions at 7 TeV showed a strong non-linear increase of the HQ multiplicity as a function of the charged particle multiplicity. We try to understand this behavior using the EPOS3 approach. Two issues play an important role: multiple scattering, in particular its impact on multiplicity fluctuations, and the collective hydrodynamic expansion. The results are very robust with respect to many details of the modeling, which means that these data contain valuable information about very basic features of the reaction mechanism in proton-proton collisions.

### I. INTRODUCTION

Although being very rare, high multiplicity events in high energy proton-proton collisions gained much attention in recent years, after discovering many features which look very much like the collective effects known from heavy ion collisions, in particular azimuthal anisotropies or the mass dependence of particle spectra. One usually studies effects as a function of the event activity, the latter one being typically the charged particle multiplicity, which takes the role of the “centrality” in heavy ion studies.

Recently, several experimental groups investigated the dependence of heavy quark production on the event activity, both for open and hidden charm or bottom. We will focus here on  $D$  meson production, where the term “ $D$  meson multiplicity” refers in the following to the average multiplicity of  $D^+$ ,  $D^0$  and  $D^{*+}$ . The ALICE collaboration found a quite unexpected result [1] as shown in fig. 1: When plotting the  $D$  meson multiplicity versus the charged particle multiplicity, both divided by the corresponding minimum bias mean values, one obtains a dependence which is very significantly more than linear, the latter one indicated by the dotted line (referred to as “diagonal”, meaning  $N_D / \langle N_D \rangle = N_{ch} / \langle N_{ch} \rangle$ ). The effect seems to be bigger for larger  $p_t$ . Both  $D$  meson and charged particle multiplicity refer to central rapidities.

Trying to understand their data, the authors of [1] analyze simulations using PYTHIA 8.157. Taking only  $D$  mesons from the hard process, the dependence on the charged particle multiplicity  $N_{ch}$  is even much less than linear, taking into account all contributions (in particular multiple scattering),

the results are close to the diagonal, slightly below for small  $p_t$  and slightly above for high  $p_t$ . So multiple scattering seems to help, it goes into the right direction, but the simulations are still far from the data.

In [1], they also refer to a percolation approach [4], which assumes that high-energy hadronic collisions are driven by the exchange of color sources between the projectile and target in the collision. These color sources have a finite spatial extension and can interact. In a high-density environment, the coherence among the sources leads to a reduction of their effective number. The source transverse mass determines its transverse size, and allows to distinguish between soft and hard sources. As a consequence, at high densities

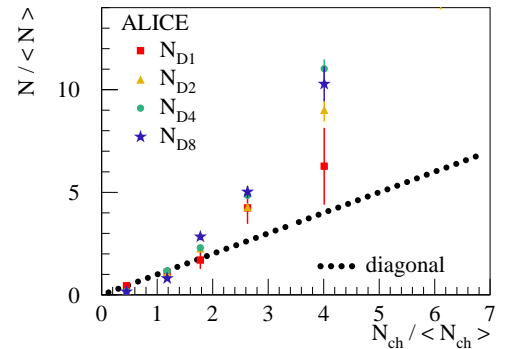


Figure 1: (Color online)  $D$  meson multiplicities versus the charged particle multiplicity, both divided by the corresponding minimum bias mean values. The different symbols and the notations  $N_{D1}$ ,  $N_{D2}$ ,  $N_{D4}$ ,  $N_{D8}$  refer to different  $p_t$  ranges: 1-2, 2-4, 4-8, 8-12 (in GeV),  $N_{ch}$  refers to the charged particle multiplicity.

the total charged-particle multiplicity, which originates from soft sources, is reduced. In contrast, hard particle production is less affected due to the smaller transverse size of hard sources. The percolation model predicts a faster-than-linear increase of heavy flavor relative production with the relative charged-particle multiplicity. However, there is no discussion the the  $p_t$  dependence.

In [1], they also show results from the multiple scattering approach EPOS3 [5]. It is a universal model, using the same scheme for pp, pA, and AA collisions, in particular a hydrodynamic expansion stage. It is shown in the paper, that EPOS without hydro get a slightly more than linear increase, with a strong enhancement when considering the hydro expansion. This is understood due to the fact that in case of hydrodynamical expansion, the multiplicity is considerably reduced compared to the case without.

Considering all these results, one may conclude (in a qualitative fashion): It seems that multiple scattering is crucial, without one would not even get close to a linear behavior. A second aspect seems to be important: A reduction of the charged particle multiplicity (rather than an increase of the  $D$  meson multiplicity) due to collective effects.

It is clear that the experimental observations are very interesting, and provide valuable insight into the very nature of the reaction mechanism in  $pp$  scattering, in particular in case of high event activity. So we try in this paper to provide a detailed analysis of the phenomenon in the EPOS3 framework. Two aspects provide the key to the understanding: Multiple scattering and collectivity.

## II. A SHORT EPOS3 SUMMARY

EPOS3 [5] is a universal model in the sense that for pp, pA, and AA collisions, the same procedure applies, based on several stages:

**Initial conditions.** A Gribov-Regge multiple scattering approach is employed (“Parton-Based Gribov-Regge Theory” PBGR [6], see Fig. 2), where the elementary object (by definition called Pomeron) is a DGLAP parton ladder, using in addition a CGC motivated saturation scale [7] for each Pomeron, of the form  $Q_s \propto N_{\text{part}} \hat{s}^\lambda$ , where  $N_{\text{part}}$  is the number of nucleons connected the Pomeron in question, and  $\hat{s}$  its energy. The parton ladders are treated as classical relativistic (kinky) strings.

**Core-corona approach.** At some early proper time  $\tau_0$ , one separates fluid (core) and escap-

ing hadrons, including jet hadrons (corona), based on the momenta and the density of string segments (First described in [8], a more recent discussion in [5]). The corresponding energy-momentum tensor of the core part is transformed into an equilibrium one, needed to start the hydrodynamical evolution, see Fig. 3. This is based on the hypothesis that equilibration happens rapidly and affects essentially the space components of the energy-momentum tensor.

**Viscous hydrodynamic expansion.** Starting from the initial proper time  $\tau_0$ , the core part of the system evolves according to the equations of relativistic viscous hydrodynamics [5, 9], where we use presently  $\eta/s = 0.08$ . A cross-over equation-of-state is used, compatible with lattice QCD [10, 11].

**Statistical hadronization.** The “core-matter” hadronizes on some hypersurface defined by a constant temperature  $T_H$ , where a so-called Cooper-Frye procedure is employed, using equilibrium hadron distributions, see [11].

**Final state hadronic cascade.** After hadronization, the hadron density is still big enough to allow hadron-hadron rescatterings. For this purpose, we use the UrQMD model [12].

The above procedure is employed for each event (event-by-event procedure).

Whereas our approach is described in detail in [5], referring to older works [6, 8, 11], we confine ourselves here to a couple of remarks, to selected items. The initial conditions are generated in the Gribov-Regge multiple scattering framework. Our formalism is referred to as “Parton-Based Gribov-Regge Theory” (PBGR [6]) and described in very detail in [6], see also [5] for all the details of the present (EPOS3) implementation. The fundamental assumption of the approach is the hypothesis that the S-matrix is given as a product of elementary objects, referred to as Pomerons. Once the Pomeron is specified (taken as a DGLAP parton ladder, including a saturation scale), everything is completely determined. Employing cutting rule techniques, one may express the total cross section in terms of cut and uncut Pomerons, as sketched in fig. 2. The great advantage of this approach: doing partial summations, one obtains expressions for partial cross sections  $d\sigma_{\text{exclusive}}$ , for particular multiple scattering configurations, based on which the Monte Carlo generation of configurations can be done. No additional approximations are needed.

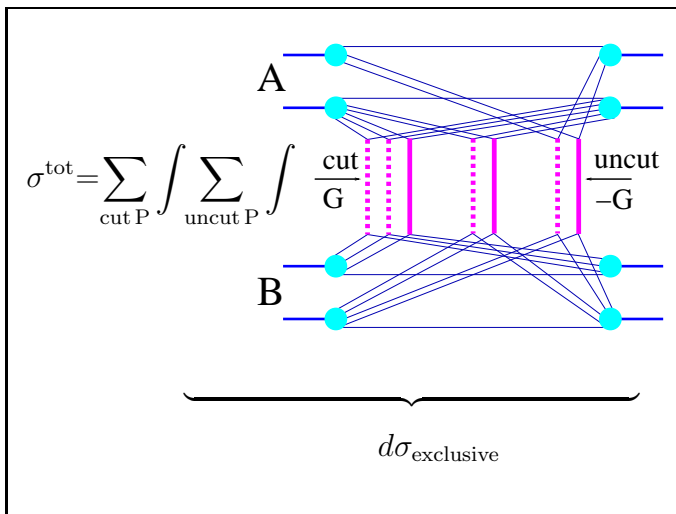


Figure 2: (Color online) PBGRT formalism: The total cross section expressed in terms of cut (dashed lines) and uncut (solid lines) Pomerons, for nucleus-nucleus, proton-nucleus, and proton-proton collisions. Partial summations allow to obtain exclusive cross sections, the mathematical formulas can be found in [6], or in a somewhat simplified form in [5].

The above multiple scattering picture is used for p-p, p-A, and A-A.

Based on the PBGRT approach, we obtain in high multiplicity  $pp$  collisions a large number of strings. The randomness of their transverse positions leads to asymmetric energy density distributions in the transverse plane at initial proper time  $\tau_0$ , as shown in the left upper plot of Fig. 3, where we show the energy density of the core for a particular (typical) event at space-time rapidity  $\eta_s = 0$ . In this example we observe an elongated (kind of elliptical) shape. The other plots in Fig. 3 show the proper time evolution of the system. Mainly due to the strong longitudinal expansion, the energy density values drop very fast. Also a transverse expansion is visible, leading first to a more symmetric shape, but then we see very clearly an expansion perpendicular to the principal axis of the initial distribution, reflecting a typical flow behavior, leading to non-zero harmonic flow coefficients and ridges in dihadron correlation functions (see [13]).

Detailed studies of  $pt$  spectra and azimuthal anisotropies (dihadron corr.,  $v_n$ ) in pp and pA can be found in [5, 14]. All parameters have been fixed, there are no more free parameters concerning the calculation discussed in this paper.

### III. HEAVY QUARK PRODUCTION IN EPOS3

Heavy quarks ( $Q$ ) are produced during the initial stage, in the PBGRT formalism, in the same way as light quarks. We have several parton ladders, each one composed of two space-like parton cascades (SLC) and a Born process. The time-like partons emitted in the SLC or the Born process are in general starting points of time like cascades (TLC). In all these processes, whenever quark-antiquark production is possible, heavy quarks may be produced. We take of course into account the modified kinematics in case of non-zero quark masses (we use  $m_c = 1.3$ ,  $m_b = 4.2$ ). In fig. 4, we show several possibilities of heavy quark production in parton ladders.

In the present work, no interactions between these initially produced heavy quarks and the fluid are considered. So all the  $D$  mesons are originating from these initial hard processes.

$D$  meson production in the EPOS3 framework has been studied extensively, comparing to data and other calculation, in ref. [15].

### IV. CORRELATING $D$ MESON AND CHARGED PARTICLE MULTIPLICITIES IN EPOS BASIC

As discussed in the introduction, we try to understand the dependence of the  $D$  meson multiplicity on the charged particle multiplicity, first for EPOS basic (without hydro). We study the case, where both multiplicities refer to central rapidities ( $|y| \leq 0.5$  for the  $D$  mesons, and  $|\eta| \leq 1$  for the charged particles). As shown in Tab. I, we use the variables  $N_{ch}$  for the charged particle multiplicity, and  $N_{D_i}$  for the  $D$  meson multiplicities for different  $p_t$  ranges. Experimental results exist as well for these particles individually, but they seem to be identical, within the error bars.

Before discussing the results of actual calculations, let us make some qualitative statements about what to expect from the basic element of the EPOS approach, namely multiple scattering. We have in each individual event a certain number of parton ladders (cut Pomerons), as shown in fig. 5. Each ladder contributes (roughly, on the average)

$N_{ch}$	Charged particle multiplicity
$N_{D1}$	D-meson multiplicity for $1 < p_t [\text{GeV}/c] < 2$
$N_{D2}$	D-meson multiplicity for $2 < p_t [\text{GeV}/c] < 4$
$N_{D4}$	D-meson multiplicity for $4 < p_t [\text{GeV}/c] < 8$
$N_{D8}$	D-meson multiplicity for $8 < p_t [\text{GeV}/c] < 12$

Table I: Definitions of the variables  $N_{ch}$  and  $N_{D_i}$ .

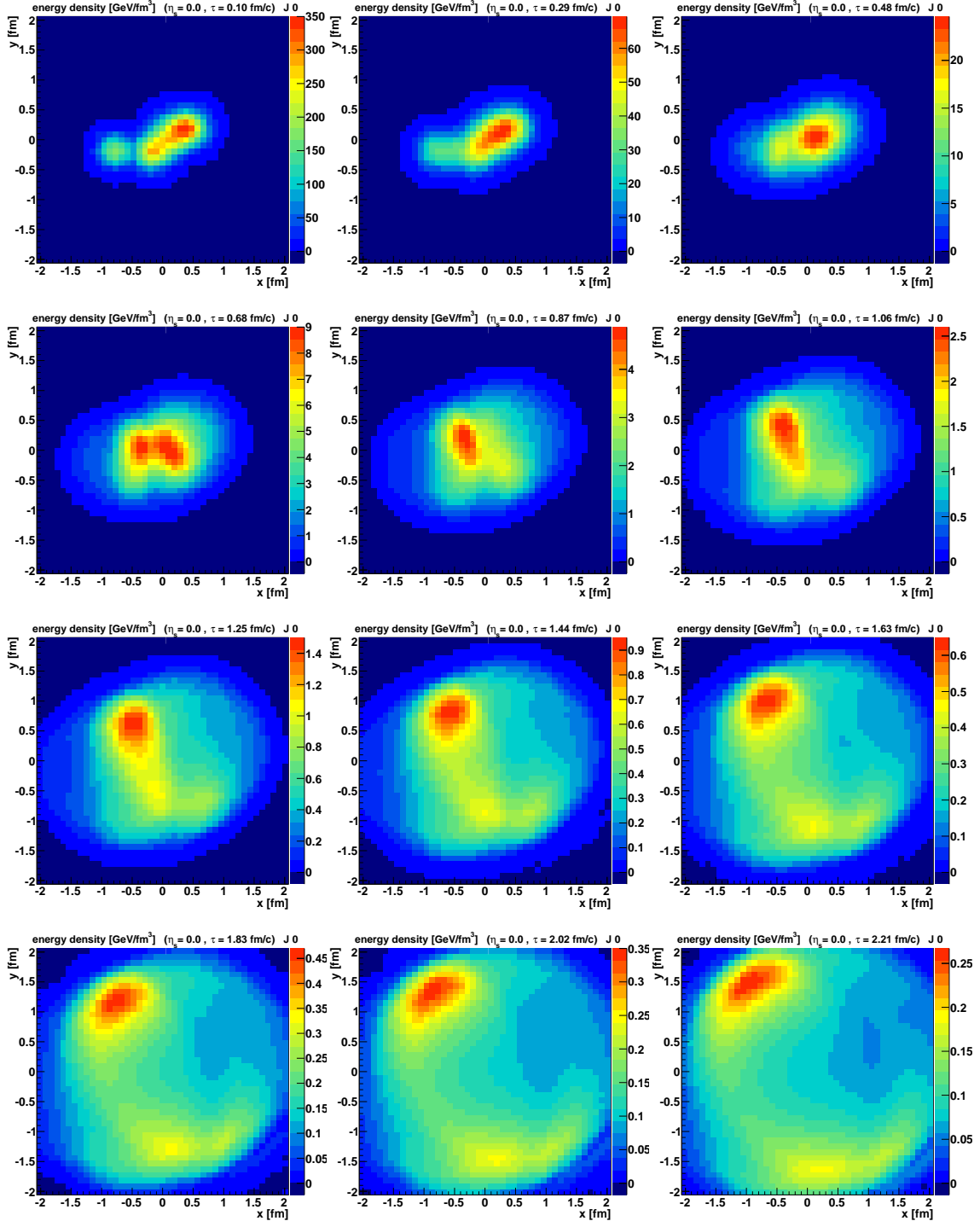


Figure 3: (Color online) Energy density distribution of the core in the transverse plane ( $x, y$  coordinates) for  $z = 0$  and for different proper times. The upper left graph corresponds to the core as obtained from the core-corona separation procedure.

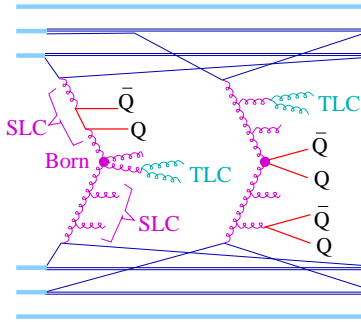


Figure 4: (Color online) Heavy quark production in EPOS3.

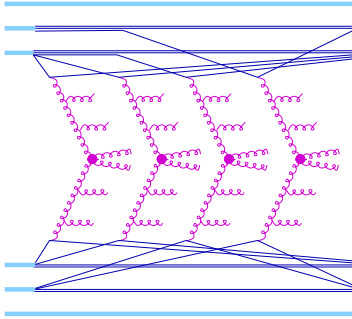


Figure 5: (Color online) An example of a multiple scattering event in EPOS: Four scatterings (parton ladders = cut Pomerons).

the same to both charged particle and charm production, so both corresponding multiplicities are proportional to the number  $N_{\text{Pom}}$  of cut Pomerons:

$$N_{Di} \propto N_{\text{ch}} \propto N_{\text{Pom}}, \quad (1)$$

which leads to a "natural" linear relation between the charged particle multiplicity  $N_{\text{ch}}$  and the  $D$  meson multiplicities  $N_{Di}$  (to first approximation). Although in reality, we will find some deviation from these first approximation results, we will use in the following nevertheless  $N_{\text{Pom}}$  as reference.

In fig. 6, we show the actual calculation of  $N_{Di}$  versus  $N_{\text{ch}}$  (in EPOS basic). Indeed a roughly linear increase is observed, as expected from eq. (1). Actually the increase is even more than linear! (in particular for large  $p_t$ ).

A more than linear increase is nice (goes into the right direction compared to data), but difficult to understand, in particular when considering fig. 7, where we plot charged and  $D$  meson multiplicities versus the Pomeron number  $N_{\text{Pom}}$ . Here,  $D$  meson multiplicities (in particular at high  $p_t$ ) increase less than  $N_{\text{ch}}$ .

How to understand a more than linear  $N_{D8}(N_{\text{ch}})$  together with the fact that  $N_{D8}$  increases much less

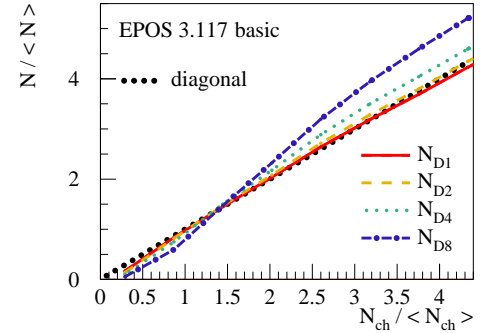


Figure 6: (Color online) The calculation of  $N_{Di}$  versus  $N_{\text{ch}}$  as obtained from EPOS basic.

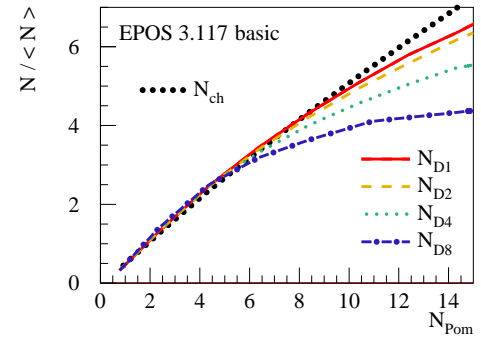


Figure 7: (Color online) Average multiplicities (of charged particles and  $D$  mesons) versus  $N_{\text{Pom}}$  as obtained from EPOS basic.

with  $N_{\text{Pom}}$  than  $N_{\text{ch}}$ ? Crucial for this discussion are fluctuations. There is certainly a strong correlation between  $N_{\text{ch}}$  and  $N_{\text{Pom}}$ , but it is not a one-to-one correspondence, as shown in a qualitative fashion in fig. 8, where we plot the number of events as a function of  $N_{\text{ch}}$  and  $N_{\text{Pom}}$ . We see a ridge, which is narrow, but finite. This results in the fact that a fixed Pomeron number  $N_{\text{Pom}}$ , which gives a particular  $N_{\text{ch}}$  as mean value, and the average Pomerons number  $N_{\text{Pom}}^*$  for a fixed value  $N_{\text{ch}}$  are not identical

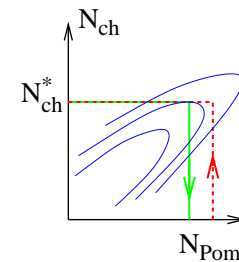


Figure 8: (Color online) Contour plot of the number of events as a function of  $N_{\text{ch}}$  and  $N_{\text{Pom}}$  (artists view).

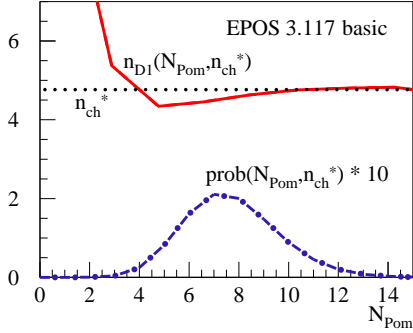


Figure 9: (Color online) Pomeron number distribution at fixed charged multiplicity,  $\text{prob}(N_{\text{Pom}}, n_{\text{ch}}^*)$  (blue line), and number  $n_{D1}(N_{\text{Pom}}, n_{\text{ch}}^*)$  of  $D$  mesons (small  $p_t$ ) for fixed  $N_{\text{Pom}}$  and  $n_{\text{ch}}^*$  as a function of the Pomeron number  $N_{\text{Pom}}$  (red line). The dotted line represents the constant value  $n_{\text{ch}}^*$ .

( $N_{\text{Pom}}^* \neq N_{\text{Pom}}$ , green and red arrows in the figure). Fig. (7) is therefore not really useful for discussing  $N_{Di}(N_{\text{ch}})$ , we have to look more into the details.

We first define normalized multiplicities,

$$n = N / \langle N \rangle, \quad (2)$$

both for charged particles ( $n_{\text{ch}}$ ) and  $D$  meson multiplicities ( $n_{D1}$ ). In the following, we consider fixed values  $n_{\text{ch}}^*$  of normalized charged multiplicities.

Consider the average normalized  $D$  meson multiplicity for the smallest  $p_t$  range, for some given  $n_{\text{ch}}^*$ , referred to as  $n_{D1}(n_{\text{ch}}^*)$ , which may be written as

$$n_{D1}(n_{\text{ch}}^*) = \sum_{N_{\text{Pom}}} \text{prob}(N_{\text{Pom}}, n_{\text{ch}}^*) \times n_{D1}(N_{\text{Pom}}, n_{\text{ch}}^*), \quad (3)$$

with  $\text{prob}(N_{\text{Pom}}, n_{\text{ch}}^*)$  being the Pomeron number distribution at fixed  $n_{\text{ch}}^*$ , and  $n_{D1}(N_{\text{Pom}}, n_{\text{ch}}^*)$  the number of  $D$  mesons for fixed  $N_{\text{Pom}}$  and  $n_{\text{ch}}^*$ . The latter two curves (as obtained from EPOS basic) are plotted in fig. 9 as a function of the Pomeron number  $N_{\text{Pom}}$  (red and blue curve) together with the constant value of  $n_{\text{ch}}^*$ , indicated by the dotted line. In the range where the Pomeron distribution is non-zero, the function  $n_{D1}(N_{\text{Pom}}, n_{\text{ch}}^*)$  is roughly constant, and even close to the value  $n_{\text{ch}}^*$ . Using this ( $n_{D1}(N_{\text{Pom}}, n_{\text{ch}}^*) \approx n_{\text{ch}}^*$ ), we get from eq. (3):

$$n_{D1}(n_{\text{ch}}^*) \approx n_{\text{ch}}^*. \quad (4)$$

The result of the exact calculation is shown in fig. 10 as red point. Also shown is the complete curve  $n_{D1}(n_{\text{ch}})$  as obtained from EPOS basic. Indeed, as indicated by eq. (4), we get an almost perfect linear increase.

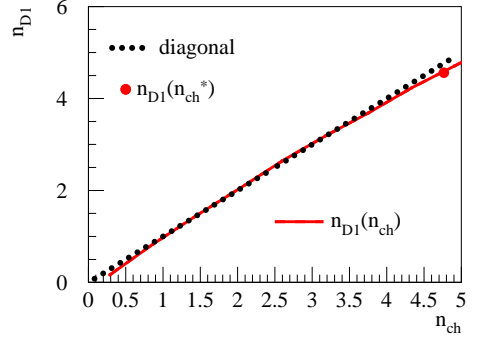


Figure 10: (Color online) Average multiplicity  $n_{D1}(n_{\text{ch}})$  of  $D$  mesons (small  $p_t$ ) as a function of  $n_{\text{ch}}$  (red line) and the diagonal ( $n_{D1} = n_{\text{ch}}$ , dotted line). The red point refers to  $n_{D1}(n_{\text{ch}}^*)$  for the particular value of  $n_{\text{ch}}^*$  used in eq. (3).

Now we will study the average normalized  $D$  meson multiplicity for the largest  $p_t$  range, for some given  $n_{\text{ch}}^*$ , which may be expressed as well in terms of the Pomeron number distribution  $\text{prob}(N_{\text{Pom}}, n_{\text{ch}}^*)$  at fixed  $n_{\text{ch}}^*$  and the number  $n_{D8}(N_{\text{Pom}}, n_{\text{ch}}^*)$  of  $D$  mesons for fixed  $N_{\text{Pom}}$  and  $n_{\text{ch}}^*$ , as

$$n_{D8}(n_{\text{ch}}^*) = \sum_{N_{\text{Pom}}} \text{prob}(N_{\text{Pom}}, n_{\text{ch}}^*) \times n_{D8}(N_{\text{Pom}}, n_{\text{ch}}^*). \quad (5)$$

The two curves representing  $\text{prob}(N_{\text{Pom}}, n_{\text{ch}}^*)$  and  $n_{D8}(N_{\text{Pom}}, n_{\text{ch}}^*)$  are shown in fig. 11. We see in the figure that  $n_{D8}(N_{\text{Pom}}, n_{\text{ch}}^*)$  increases strongly towards small  $N_{\text{Pom}}$  with an increasing slope. Let us compare the expression of eq. (5) with the corresponding sum (as a reference) where we

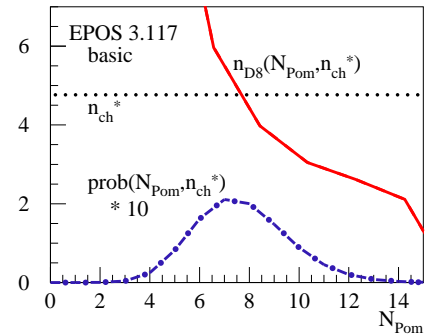


Figure 11: (Color online) Pomeron number distribution at fixed charged multiplicity,  $\text{prob}(N_{\text{Pom}}, n_{\text{ch}}^*)$  (blue line), and number  $n_{D8}(N_{\text{Pom}}, n_{\text{ch}}^*)$  of  $D$  mesons (large  $p_t$ ) for fixed  $N_{\text{Pom}}$  and  $n_{\text{ch}}^*$  as a function of the Pomeron number  $N_{\text{Pom}}$  (red line). The dotted line represents the constant value  $n_{\text{ch}}^*$ .

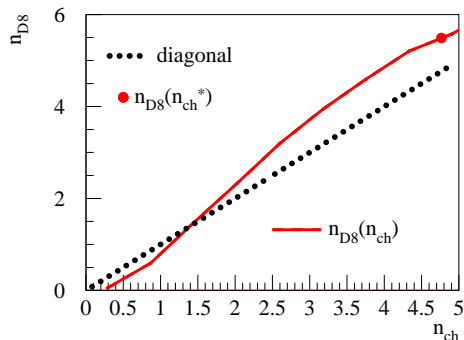


Figure 12: (Color online) Average multiplicity  $n_{D8}(n_{ch})$  of  $D$  mesons (large  $p_t$ ) as a function of  $n_{ch}$  (red line) and the diagonal ( $n_{D1} = n_{ch}$ , dotted line). The red point refers to  $n_{D8}(n_{ch}^*)$  for the particular value of  $n_{ch}^*$  used in eq. (5).

use  $n_{D8}(N_{Pom}, n_{ch}^*) = n_{ch}^*$ , which would lead to  $n_{D8}(n_{ch}^*) = n_{ch}^*$ . For large  $N_{Pom}$ , the contribution to the sum in eq. (5) will be less than the reference case, but this is more than compensated at small  $N_{Pom}$ . Therefore, we have

$$n_{D8}(n_{ch}^*) > n_{ch}^*, \quad (6)$$

which is confirmed by the precise calculation shown in fig. 12 as red point. Also shown is the complete curve  $n_{D8}(n_{ch})$  as obtained from EPOS basic. Indeed, as indicated by eq. (6), we get a more than linear increase.

Let us summarize the main points of the preceding discussion:

- The number of Pomerons fluctuates for given charged multiplicity.
- The multiplicity  $N_{D8}$  of high transverse momentum  $D$  mesons increases strongly towards small  $N_{Pom}$  for given multiplicity, which simply means that it is favored to produce high  $p_t$   $D$  mesons for fewer (and more energetic) Pomerons.
- This leads to a more than linear increase of the  $D$  meson multiplicity as a function of the charged particle one.
- The effect is absent for low  $p_t$   $D$  mesons, which show a linear increase.

The results of our calculation agree qualitatively with the trend in the data, namely a more than linear increase, in particular for high transverse momentum  $D$  mesons. But the effect is actually too small, as seen in fig. 13, where we plot the  $D$  meson multiplicities versus the charged particle multiplicity, both for our calculation and data from ALICE [1].

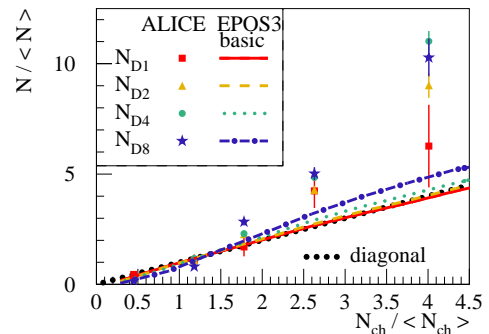


Figure 13: (Color online)  $D$  meson multiplicities versus the charged particle multiplicity, both divided by the corresponding minimum bias mean values. The different symbols and the notations  $N_{D1}$ ,  $N_{D2}$ ,  $N_{D4}$ ,  $N_{D8}$  refer to different  $p_t$  ranges: 1-2, 2-4, 4-8, 8-12 (in GeV),  $N_{ch}$  refers to the charged particle multiplicity. We compare our calculation from EPOS basic (lines) to ALICE data (points).

## V. THE INFLUENCE OF THE HYDRODYNAMICAL EVOLUTION

As seen in the previous chapter, we do see a more than linear increase of  $n_{Di}(n_{ch})$  in EPOS basic, but the effect is too small. But anyhow, EPOS basic (w/o hydro) reproduces neither spectra nor correlations, we have to consider the full approach, i.e. EPOS with hydrodynamical evolution (with or without hadronic cascade makes no difference). In fig. 14, we plot again the  $D$  meson multiplicities versus the charged particle, EPOS3 compared to data, but here we refer to the calculations based on the full EPOS model (with hydro). We see a significant non-linear increase, much more pronounced as in the case of EPOS basic (without hydro).

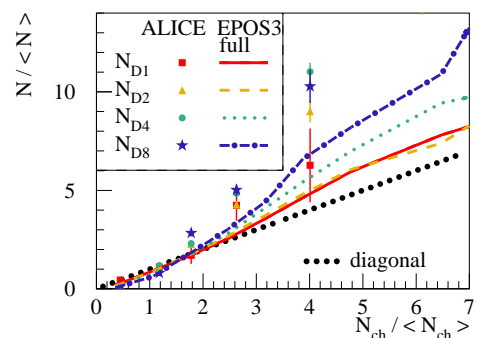


Figure 14: (Color online) Same as fig. 13, but here we show the calculations based on the full EPOS model (with hydro).

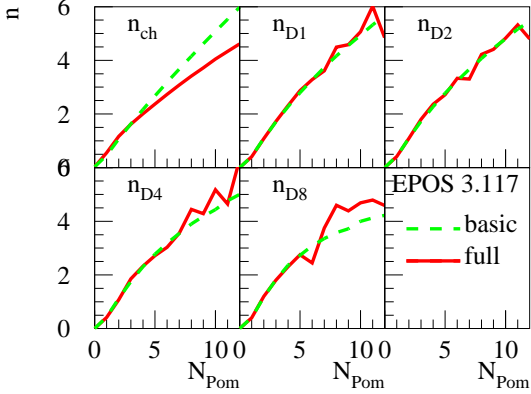


Figure 15: (Color online) Average normalized multiplicities (of charged particles and  $D$  mesons) versus  $N_{\text{Pom}}$  obtained from EPOS basic (dashed green lines) as compared to full EPOS (full red lines).

How can we understand this increased non-linearity, due to the hydrodynamical evolution? This is what we are going to discuss in the following.

In fig. 15, we plot the average normalized multiplicities  $n_{\text{ch}}$  and  $n_{D_i}$  as a function of the Pomeron number  $N_{\text{Pom}}$ . We compare the results from EPOS basic and the full EPOS approach. As expected, for the  $D$  meson multiplicities the two calculations are identical, due to the fact that the hydrodynamical evolution does not affect  $D$  meson production. The situation is quite different concerning the charged particle multiplicities: Here, the multiplicities from full EPOS (including hydro) are considerably below the results from EPOS basic (without hydro). This makes a big effect, and leads to a significant non-linear increase of the  $D$  meson multiplicities versus the charged particle multiplicity. But important to keep in mind:

- Not the charm production is increased with increasing “collision activity” (Pomeron number),
- but the charged particle multiplicity is reduced when including a hydrodynamical expansion.

Why do we have such a multiplicity reduction due to the hydrodynamical evolution? To understand this, we compare in fig. 16 the transverse momentum spectra of charged particles for two different scenarios:

- Particle production in a hydrodynamical scenario, as used in full EPOS, but with vanishing transverse flow, and

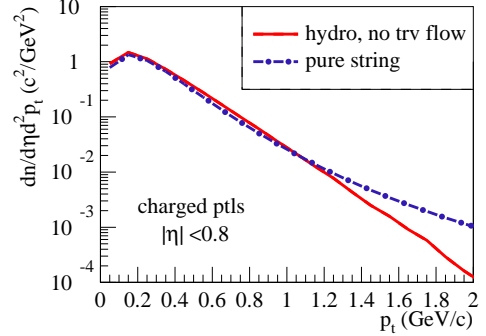


Figure 16: (Color online) Transverse momentum spectra of charged particles in a hydrodynamical scenario but with vanishing transverse flow (red solid line), and from string fragmentation (blue dashed-dotted line).

- Particle production from string fragmentation, as in EPOS basic.

It can be seen that at small transverse momentum the two scenarios give identical results (by accident). From this, we understand that in a full hydrodynamical scenario with a strong transverse flow, part of the available energy goes into flow rather than particle production, reducing the multiplicity.

## VI. TRANSVERSE MOMENTUM DEPENDENCE

Why is the non-linearity of  $N_{D_i}(N_{\text{ch}})$  more pronounced at high  $p_t$ ? The naive expectation would be that the  $N_{\text{ch}}$  reduction should affect all  $D$  meson  $p_t$  ranges in the same way. But again we have to look more into the details.

We remember the arguments related to fig. 11, where we plotted (for EPOS basic) the Pomeron number distribution  $\text{prob}(N_{\text{Pom}}, n_{\text{ch}}^*)$  at fixed charged multiplicity and the number  $n_{D8}(N_{\text{Pom}}, n_{\text{ch}}^*)$  of  $D$  mesons (large  $p_t$ ) for given  $N_{\text{Pom}}$  and  $n_{\text{ch}}^*$ , as a function of the Pomeron number  $N_{\text{Pom}}$ . We could understand the non-linear increase of  $n_{D8}(n_{\text{ch}})$  to be due to fluctuations of the Pomeron numbers for fixed  $n_{\text{ch}}^*$  in connection with a strong increase of  $n_{D8}(N_{\text{Pom}}, n_{\text{ch}}^*)$  towards small  $N_{\text{Pom}}$  ( $D$  production is favored when having fewer but more energetic Pomerons). We shown in fig. 17 the same curves again (left plot) together with the corresponding curves for full EPOS (right plot). We use the same fixed value of charged particle multiplicity for the two scenarios ( $N_{\text{ch}}^*(\text{full}) = N_{\text{ch}}^*(\text{basic})$ ), which leads to a somewhat bigger normalized multiplicity in case of full EPOS



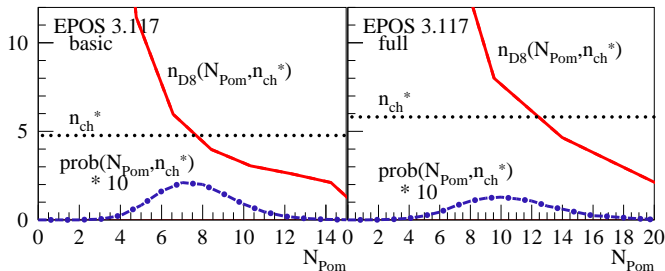


Figure 17: (Color online) Pomeron number distribution at fixed charged multiplicity (blue dashed-dotted lines), the number of  $D$  mesons (large  $p_t$ ) at fixed charged multiplicity as a function of  $N_{\text{Pom}}$  (red full line), and the constant values of the charged multiplicity (black dotted lines). We show results for EPOS basic (left plot) and full EPOS (right plot).

( $n_{\text{ch}}^*(\text{full}) > n_{\text{ch}}^*(\text{basic})$ ). We see that including hydro leads to a shift towards bigger values and a broadening of the Pomeron distribution. In addition, the curve  $n_{D8}(N_{\text{Pom}}, n_{\text{ch}}^*)$  crosses the constant  $n_{\text{ch}}^*$  line even above the maximum of the Pomeron number distribution. These two features enhance the effect (the non-linearity) observed already for EPOS basic. For small transverse momenta this “hydro-enhancement” of the effect is absent (we do not have any increase of  $n_{D1}(N_{\text{Pom}}, n_{\text{ch}}^*)$  towards small  $N_{\text{Pom}}$ ).

## VII. TAKING CHARGED PARTICLE MULTIPLICITY AT LARGE RAPIDITIES

We are still interested in the correlation of  $D$  meson and charged particle multiplicity, but here we consider the multiplicity at large pseudo-rapidities, namely in the intervals  $2.8 < \eta < 5.1$  and  $-3.7 < \eta < -1.7$ , which correspond to the Vzero detectors in ALICE. We refer to the corresponding multiplicity as “Vzero multiplicity” using the symbol  $N_{vz}$ , and  $n_{vz}$  for the normalized multiplicity. The multiplicity  $n_{\text{ch}}$  at central pseudo-rapidities, discussed in the previous chapter, will be referred to as “central multiplicity”. In fig. 18, we plot the  $D$  meson multiplicity  $N_{D4}$  versus the Vzero multiplicity (red solid line) and versus the central multiplicity (blue dashed line). We show results from ALICE (left plot) and from full EPOS simulations (right plot). Clearly visible is the fact that (in both, data and simulation) the non-linear increase is considerably reduced in case of Vzero multiplicity compared to the central multiplicity. So it seems to matter whether the charged particle multiplicity is considered in the

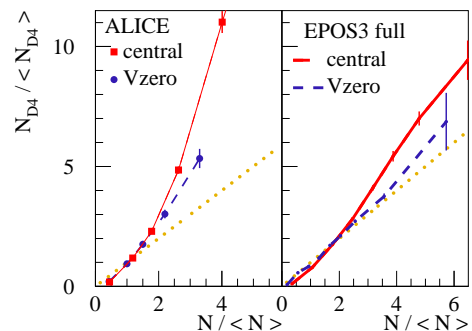


Figure 18: (Color online)  $D$  meson multiplicity  $N_{D4}$  versus the Vzero multiplicity (red solid lines) and versus the central multiplicity (blue dashed lines). We show results from ALICE (left plot) and from full EPOS simulations (right plot).

same rapidity range as the  $D$  meson multiplicity or not.

How to understand this? Is there less “hydro effect” in case of the Vzero multiplicity? The answer is “no”, as can be seen in fig. 19. We see that also in the case of Vzero multiplicity, there is a strong suppression of the multiplicity when considering hydrodynamical flow. So the “flow effect” is the same for central and Vzero multiplicities.

But the flow effect is only half of the story, it increases a primary effect due to Pomeron number fluctuations. We therefore plot in fig. 20, the Pomeron number distribution at fixed charged multiplicity and number of  $D$  mesons (large  $p_t$ ) for fixed  $N_{\text{Pom}}$  and fixed charged particle multiplicity, as a function of the Pomeron number  $N_{\text{Pom}}$  for the two cases, namely “central multiplicity” (left) and

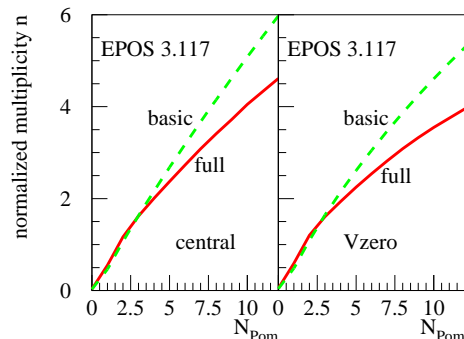


Figure 19: (Color online) Average normalized charged particle multiplicity versus  $N_{\text{Pom}}$  obtained from EPOS basic (dashed green lines) as compared to full EPOS (full red lines). We show results for the “central” multiplicity (left) and the Vzero multiplicity (right).

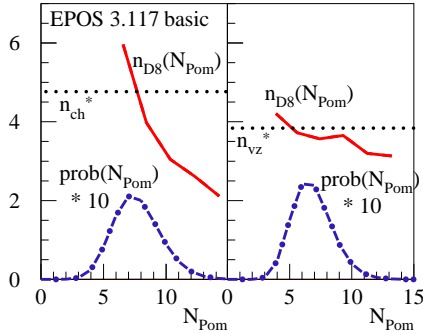


Figure 20: (Color online) Pomeron number distribution at fixed charged multiplicity (dashed-dotted blue lines) and number of  $D$  mesons (large  $p_t$ ) for fixed  $N_{Pom}$  and fixed charged particle multiplicity (solid red lines) as a function of the Pomeron number  $N_{Pom}$ . The dotted line represents the constant charged particle multiplicity. We show results for the “central multiplicity” (left) and the “Vzero multiplicity” (right).

the “Vzero multiplicity” (right). Whereas  $n_{D8}$  increases strongly towards small  $N_{Pom}$  in the case of “central multiplicity”, the corresponding curve for the “Vzero multiplicity” (right plot) is almost flat, providing an essentially linear increase of  $n_{D8}(n_{vz})$ . The secondary effect due to the hydro evolution will provide some non-linearity, but less pronounced as compared to the case of central multiplicity, as seen in fig. 18 (right plot, blue dashed line). So the main difference between the case of “central multiplicity” (left) and the “Vzero multiplicity” is the fact that the latter is uncorrelated with respect to the  $D$  meson multiplicity.

### VIII. SUMMARY

We analyzed the dependence of  $D$  meson multiplicities (in different  $p_t$  ranges) on the charged

particle multiplicity in proton-proton collisions at 7 TeV, using the EPOS3 approach. We find a non-linear increase. Two issues play an important role: Multiplicity fluctuations due to multiple scattering (realized via multiple Pomerons), and the collective hydrodynamic expansion. Multiplicity fluctuations are important since in particular high  $p_t$   $D$  meson production at given (large) charged particle multiplicity is very much enhanced for small Pomeron numbers, which is responsible for the strong increase of the  $D$  meson production with multiplicity. In addition, the effect is amplified when turning on the hydrodynamical expansion, due to a reduction of the charged particle multiplicity with respect to the model without hydro. The non-linearity is reduced when considering multiplicities at large pseudo-rapidities, not competing with  $D$  meson production. Our results are very robust with respect to many details of the modeling (and not just specific to EPOS3), they essentially depend on very basic features of the reaction mechanism in proton-proton collisions, namely having multiple scattering and a multiplicity reduction due to collective effects. The data discussed in this paper contain therefore valuable information.

### Acknowledgments

This research was carried out within the scope of the GDRE (European Research Group) “Heavy ions at ultrarelativistic energies”. B.G. acknowledges the financial support by the TOGETHER project of the Region of “Pays de la Loire”. B. G. gratefully acknowledges generous support from Chilean FONDECYT grants 3160493.

- 
- [1] ALICE collaboration, arXiv:1505.00664v1
  - [2] T. Sjostrand, S. Mrenna, and P. Z. Skands, JHEP 0605 (2006) 026, arXiv:hep-ph/0603175 [hep-ph].
  - [3] T. Sjostrand, S. Mrenna, and P. Z. Skands, Comput.Phys.Commun. 178 (2008) 852–867, arXiv:0710.3820
  - [4] E. Ferreira and C. Pajares, arXiv:1501.03381.
  - [5] K. Werner, B. Guiot, I. Karpenko, and T. Pierog, Phys.Rev. C89 (2014) 064903, arXiv:1312.1233.
  - [6] H. J. Drescher, M. Hladik, S. Ostapchenko, T. Pierog and K. Werner, Phys. Rept. 350, 93, 2001
  - [7] L. McLerran, R. Venugopalan, Phys. Rev. D 49 (1994) 2233; L. McLerran, R. Venugopalan, Phys. Rev. D 49 (1994) 3352; L. McLerran, R. Venugopalan, Phys. Rev. D 50 (1994) 2225.
  - [8] K. Werner, Phys. Rev. Lett. 98, 152301 (2007)
  - [9] Iu. Karpenko, P. Huovinen, M. Bleicher, arXiv:1312.4160
  - [10] S. Borsanyi et al., JHEP 1011 (2010) 077, arXiv:1007.2580
  - [11] K. Werner, Iu. Karpenko, T. Pierog, M. Bleicher, K. Mikhailov, arXiv:1010.0400, Phys. Rev. C 83, 044915 (2011)
  - [12] M. Bleicher et al., J. Phys. G25 (1999) 1859; H. Pe-

- tersen, J. Steinheimer, G. Burau, M. Bleicher and H. Stoecker, Phys. Rev. C78 (2008) 044901
- [13] K. Werner, Iu. Karpenko, T. Pierog, Phys.Rev.Lett. 106 (2011) 122004, arXiv:1011.0375
- [14] K. Werner, M. Bleicher, B. Guiot, Iu. Karpenko, T. Pierog, Phys.Rev.Lett. 112 (2014) 23, 232301, arXiv:1307.4379
- [15] B. Guiot, Ph.D. Thesis, University of Nantes, 2014